An Assessment of the Current WAAS Ionospheric Correction Algorithm in the South American Region

Attila Komjathy, Lawrence Sparks, Anthony J. Mannucci and Xiaoqing Pi

NASA Jet Propulsion Laboratory/ California Institute of Technology
M/S 238-600, 4800 Oak Grove Drive, Pasadena, CA 91109

BIOGRAPHIES

Attila Komjathy is currently a staff member of the Ionospheric and Atmospheric Remote Sensing (IARS) Group of the Tracking Systems and Applications Section at NASA s Jet Propulsion Laboratory (JPL), specializing in remote sensing techniques using the Global Positioning System. Prior to his joining JPL in July 2001, he worked on the utilization of GPS reflected signals as a Research Associate at the University of Colorado's Center for Astrodynamics Research. He received his Ph.D. from the Department of Geodesy and Geomatics Engineering of the University of New Brunswick, Canada in 1997.

Lawrence Sparks is a senior member of the IARS Group at JPL. He received his Ph.D. in Applied Physics from Cornell University. His published research has spanned fields including fusion plasma physics, solar magneto-hydrodynamics, atmospheric radiative transfer, and ionospheric modeling. He is currently working on applications of GPS to ionospheric science.

Anthony J. Mannucci is supervisor of the IARS Group at JPL. He has developed ionospheric calibration systems for deep space tracking and Earth science applications. He works with the Federal Aviation Administration on the Wide Area Augmentation System differential GPS implementation and is a member of the international ionospheric working group for Satellite-Based Augmentation Systems (SBAS). He obtained a Ph.D. in Physics from U.C. Berkeley in 1989.

Xiaoqing Pi is a senior member of the Ionospheric and Atmospheric Remote Sensing Group at JPL. He is also an associate research professor in the Mathematics Department of the University of Southern California. He received a Ph.D in astronomy from Boston University. He has been involved in the research and development of ionospheric applications of GPS, ionospheric modeling, and ionospheric storms, irregularities and scintillation. He is currently working on ionospheric data assimilation models, satellite-based augmentation systems, and ionospheric scintillation of GPS signals.

ABSTRACT

The Federal Aviation Administration s (FAA) Wide Area Augmentation System (WAAS) for civil aircraft navigation is focused primarily on the Conterminous United States (CONUS). The ionospheric correction algorithms for WAAS have been characterized extensively for this mid-latitude region of the ionosphere where benign conditions usually exist. Researchers are facing a more formidable challenge in addressing the ionospheric impact on navigation using Satellite-Based Augmentation Systems (SBAS) in other parts of the world such as the South American region. At equatorial latitudes, geophysical conditions lead to the so-called Appleton-Hartree (equatorial) anomaly phenomenon, which results in significantly larger ionospheric range delays and range delay spatial gradients than is observed in the CONUS region.

In this paper, we use data from the South American region to perform a preliminary quantitative assessment of the performance of WAAS correction algorithms in this region. For this study, we accessed a world-wide network of 230 dual-frequency GPS receivers. The network includes: 1) the Continuously Operating Reference Sites (CORS) in the United States; 2) stations in and near South America as part of the Brazilian Network of Continuous Monitoring of GPS (RBMC), operated by the Brazilian Institute of Geography and Statistics

(IGBE); and (3) sites included in the International GPS Service (IGS) global network. Data sets have been selected to include both a quiet and geomagnetically disturbed day. To provide ground-truth and calibrate GPS receiver and transmitter inter-frequency biases, we processed the GPS data using Global Ionospheric Mapping (GIM) software developed at the NASA Jet Propulsion Laboratory to compute calibrated high resolution observations of ionospheric total electron content (TEC).

We assessed the WAAS s planar fit algorithm in the equatorial region where the spatial gradients and the absolute slant TEC are known to be the highest in the world. We found that in Brazil the dominant error source for the WAAS planar fit algorithm is the inherent spatial variability of the equatorial ionosphere with ionospheric slant range delay residuals as high as 15 meters and root-mean square residuals for the quiet day of 1.9 meters. This compares to a maximum residual of 2 meters in CONUS, and 0.5 meter RMS. We revealed that ionospheric gradients in Brazil are at the 2 meter over 100 km level. Contrary to results obtained for CONUS, we discovered that a major ionospheric storm had a small impact on the planar fit residuals in Brazil.

INTRODUCTION

The Wide-Area Augmentation System (WAAS) developed for the Conterminous United States (CONUS) is only one the several Space-Based Augmentation Systems (SBAS) under consideration worldwide. Other SBAS developments are under way in Europe, Japan, India and Brazil.

Relatively benign ionospheric conditions in the mid-latitude CONUS region are compatible with accurate ionospheric range corrections for WAAS. Providing ionospheric corrections for Brazil is significantly more challenging, since ionospheric range delays and range delay spatial gradients are among the largest in the world in the absence of ionospheric storms (during infrequent ionospheric storms, even mid-latitude regions present challenging conditions). In summary, the ionosphere in the Brazilian sector shows significantly different behavior from that of the mid-latitude sector.

The ionosphere has been extensively studied to support WAAS at the CONUS sector. The published literature discussing ionospheric corrections for WAAS in the CONUS is extensive; see e.g. Enge et al., [1996], WAAS MOPS [1999], Walter et al., [2000] and Sparks et al., [2002]. Various alternative ionospheric correction algorithms have been presented by e.g., Hansen et al., [1997], Sparks et al., [2000] and Blanch et al., [2002]. A potential application of WAAS algorithms to Brazil has recently been investigated by Klobuchar et al., [2002] using simulated data. The temporal and spatial variability of the low-latitude ionosphere was studied in the context of ionospheric storms by e.g., Dehel and Corbelli [2002] and Fedrizzi et al., [2000] using a network of dual-frequency GPS receivers in Brazil. Investigating the possible application of the current WAAS algorithm using actual GPS data is the natural progression of the previous studies and therefore the main focus of this paper.

In this research, we first review the estimation method used to solve for inter-frequency biases (nuisance parameters) in the GPS satellites and receivers using a global network of 230 GPS sites in order to provide ground truth data for the analysis. Subsequently, we describe the WAAS planar fit algorithm used to estimate the vertical ionospheric range delay at fixed latitude/longitude locations known as ionospheric grid points (IGPs). We examine the implications of using the currently adopted WAAS algorithm in Brazil and compare ionospheric range residuals using receivers in the CONUS with that of Brazilian stations. We characterize a number of error sources affecting the computed ionospheric range delays.

GIM BIAS ESTIMATION STRATEGY

To provide ground-truth, we used the Global Ionospheric Mapping (GIM) software developed at the NASA Jet Propulsion Laboratory [Mannucci et al., 1998] to compute high precision slant ionospheric delay by removing the satellite and receiver differential biases from the ionospheric observables, generated from carrier-phase data adjusted to match the ionospheric delay based on dual-frequency pseudoranges. The estimation of the satellite and receiver biases is described here briefly.

Ionospheric measurements from a GPS receiver can be modeled with the well-known single-shell ionospheric model using the following observation equation [see e.g. Mannucci et al., 1999 and Komjathy et al., 2002]:

$$TEC = M(h,E)\sum_i C_i B_i(lat,lon) + b_r + b_s \ , \qquad (1)$$

where

TEC is the slant Total Electron Content measured by the linear combination of the GPS dual-frequency carrier phase and pseudorange ionospheric observables, typically expressed in TEC units. One TEC Unit (10^{16}electron/m^2) corresponds to about 0.163 meter ionospheric delay at the L1 frequency,

$M(h,E)$ is the thin-shell mapping function for ionospheric shell height h and satellite elevation angle E (for the definition of the thin-shell geometric mapping function see e.g. Mannucci et al., [1998] or Komjathy [1997],

$B_i(lat, lon)$ are horizontal basis functions (based on, for example, bicubic splines or bilinear interpolants) evaluated at the ionospheric pierce point (IPP) – the intersection of the ray path of a signal propagating from the satellite to the receiver with a thin spherical shell – located at latitude *lat* and longitude *lon* on the thin shell,

C_i are basis function coefficients (real numbers),

b_r, b_s are the satellite and receiver differential biases, assumed constant over periods of 24 hours or more.

The dependence of vertical TEC on latitude and longitude is parameterized as a linear combination of the two-dimensional basis functions B_i which are functions of solar-geomagnetic longitude and latitude [Mannucci et al., 1998] (We note that the summation in Equation 1 is over all basis functions B_i). Using the carrier phase-leveled ionospheric GPS observables, a Kalman filter simultaneously solves for the instrumental biases and the coefficients C_i which are allowed to vary in time as a random walk stochastic process [Iijima et al., 1999]. The basis functions currently used are based on a bicubic spline technique developed at JPL [Lawson, 1984].

Although the main focus of this research is the comparison between CONUS and Brazilian sectors, we decided to use a global network of some 230 stations to solve for high precision satellite and receiver differential biases that are used to correct the measurements. Research has shown that the most reliable satellite bias estimates can be achieved when using the data strength of a global network of GPS receivers instead of regional GPS networks [Komjathy, 1997]. We note that the WAAS system itself uses a similar estimation scheme for biases applied over the regional WAAS network.

WAAS PLANAR FIT IONOSPHERIC MODEL

In the currently implemented WAAS ionospheric real-time correction algorithm, the vertical ionospheric delay is estimated at each ionospheric grid point (IGP) by constructing a planar fit to a set of (bias-corrected) slant measurements projected to vertical:

$$TEC = M(h,E)\left[a_0 + a_1 d_E + a_2 d_N\right] , \qquad (2)$$

where

a_0, a_1, a_2 are the planar fit parameters,

d_E, d_N are the distances from the IGP to the IPP in the eastern and northern directions, respectively.

Each least squares fit includes all IPPs that lie within a minimum fit radius surrounding the IGP. If the number of IPPs within this minimum radius is less than N_{min}, the fit radius R_{fit} is extended until it encompasses N_{min} points. In this study we do not tabulate data when the fit radius is increased to its maximum value of R_{max} without having reached N_{min} points. Due to the high spatial variability of the ionosphere at low latitudes, R_{max} was chosen to be 500 km, which is significantly smaller than the value being used for WAAS (2100 km in the current implementation). When ionospheric spatial gradients are large, we expect smaller fit radii to provide higher accuracy (experience tuning the WAAS algorithms in CONUS tends to confirm this). The disadvantage of using smaller radii is that it lowers the number of points in the fit, which may lower integrity of the corrections. However, the focus of this initial study is relative accuracy of ionospheric corrections between low and mid-latitudes. We wanted to obtain as good results as is practical with the planar fit at low latitudes, which suggests using small fit radii. We used the same 500 km value for R_{max} in our assessment of the residuals in CONUS.

In our WAAS estimation scheme (see Equation 2), we did not solve for the satellite and receiver differential biases. Instead, we used the GIM approach, outlined in Equation 1 to solve for high precision differential biases and calibrated the ionospheric range measurements before applying Equation 2. This is similar to the approach used in the WAAS.

DATA ANALYSIS STRATEGY

In our data analysis, we treated every IPP data point as if it were collocated with a WAAS IGP (so-called pseudo IGP approach). Subsequently, we applied the WAAS planar fit ionospheric model algorithm to estimate the vertical ionospheric delays at each of these IPPs, treated as pseudo IGP values. Starting with the set of measurements that contributed to the planar fit, we then computed the residual difference between the slant measurements and the estimated slant delays based on the planar fit, projecting the vertical TEC from the planar estimate into the line-of-site using the WAAS thin-shell obliquity factor. This residuals analysis provides a measure of the performance of the planar fit algorithm in reproducing slant TEC for the user.

To investigate how ionospheric spatial gradients contribute to errors in the WAAS corrections in the CONUS and the Brazilian sectors, we looked at pairs of GPS receivers observing the same satellites at nearly identical elevation and azimuth angles. Vertical delay differences were computed after projecting the slant ionospheric range delay into the vertical. See Figure 1.

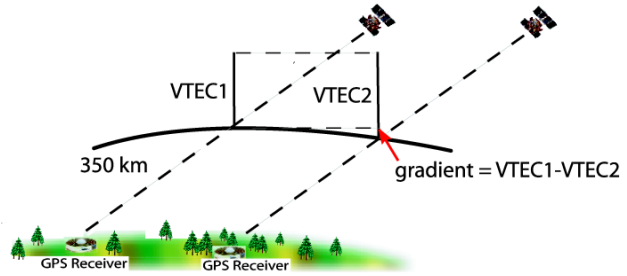

Figure 1. Illustration for computing ionospheric delay differences versus distance (gradient) for separated measurements with similar look angles.

We were also interested in finding out the potential range errors introduced by using the WAAS thin-shell mapping function in Brazil. To do that we analyzed measurements for which the IPPs were nearly co-located but differed in elevation angle. Mapping function errors were computed by taking the difference between the two slant ionospheric measurements, each projected to the vertical using the WAAS thin-shell mapping function.

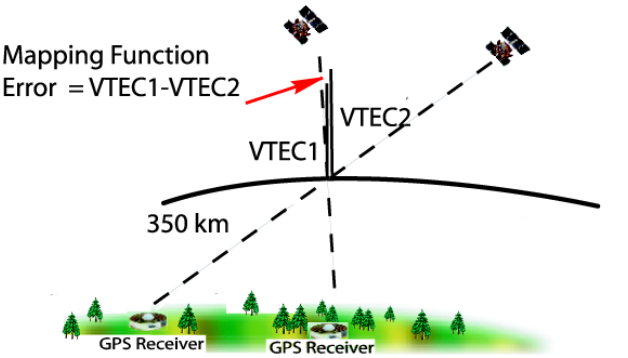

Figure 2. Illustration for computing mapping function error. Measurements with nearly collocated IPPs were differenced.

DATA SETS

For our test data set, we chose a quiet and a storm day, 30 March and 31 March 2001, respectively, using GPS receivers from the Continuously Operating Reference Stations (CORS) network, maintained by the US National Geodetic Survey [CORS, 2002], the International GPS Service [IGS, 2002], and the Brazilian Network for Continuous Monitoring of GPS (RBMC). In Figure 3, we show the Kp and DST indices for a period in 2001 indicating a major storm in March 31.

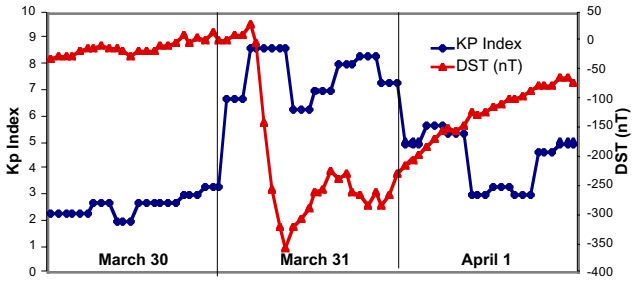

Figure 3. Behavior of Kp and Dst indices during the focus period in March. Negative excursions in Dst indicate increased ring current in the Earth s magnetosphere brought on by geomagnetic disturbances. Increases in Kp index indicate enhanced geomagnetic activity at a number of globally-distributed magnetic observatories.

In Figure 4. we show the global distribution of the GPS reference stations for March 31. The small filled circles in red represent the 230 sites that were used to provide unbiased line-of-site TEC ground-truth data. The larger circles in blue indicate the CONUS and Brazilian sectors from which stations were used for the residual analysis.

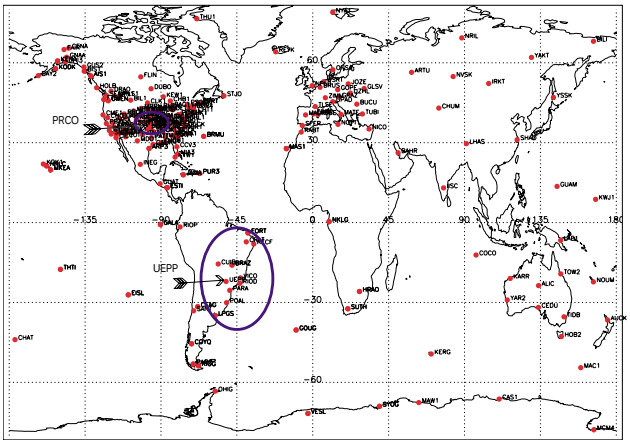

Figure 4. Network of CORS, IGS and RBMC stations processed for March 30–31, 2001.

ANALYSIS OF RESULTS

First we calibrated the satellite and receiver differential biases using the GIM method and data from the global network. Subsequently, we selected the GPS sites in Brazil and the same number of GPS sites in the CONUS sector to study the residuals when the same WAAS algorithm is applied to both middle and low-latitude sites.

Comparison of CONUS and Brazilian planar fit residuals for quiet day. We selected one station from CONUS (PRCO at Purcell, Oklahoma) and another one in Brazil (UEPP at Sao Paulo, Brazil) to illustrate typical behavior of the slant ionospheric delays and residuals to the planar fit. (See Figure 4 for stations PRCO and UEPP indicated with arrows). Note that the residuals (scale on the right) are all plotted in the slant domain. To compute residuals, the fitted vertical TEC value at an IPP location was converted to slant and differenced with the slant TEC measurement. We looked at several sites and concluded that PRCO and UEPP are representative for middle and low latitude conditions.

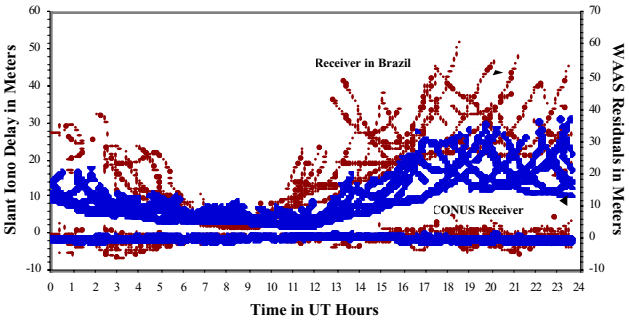

Figure 5. Ionospheric slant delays for a typical CONUS (blue) and Brazilian (red) station for the quiet day March 30, 2001. Slant-range residuals to the planar fit are also shown.

In Figure 5, we find that slant range ionospheric delays for CONUS range between 0 and 38 meters for this high solar activity period, whereas in the low-latitude sector the highest values can be as much as 52 meters (an elevation cutoff angle of 10 degrees was used throughout this analysis). In the second Y axis, we also indicate the WAAS planar fit residuals (difference between slant measurement and fitted vertical delay converted to slant). For the geo-magnetically quiet day, we find that WAAS planar fit slant residuals never exceed 2 meters for CONUS, but reach as high as 8 meters for station UEPP in Brazil.

The slant range residuals are re-plotted in Figure 6, this time as a function of elevation angle, for CONUS (in blue) and Brazil (in red). It is interesting that the spatial variability of the equatorial ionosphere is so high that we cannot see a clear elevation angle dependence in the Brazilian residuals. However, the elevation angle dependence of these residuals is quite pronounced in the CONUS. Generally, we would expect the residuals to grow with lower elevation angle since the additional path length through the ionosphere at lower elevations increases the range delay by up to a factor of three.

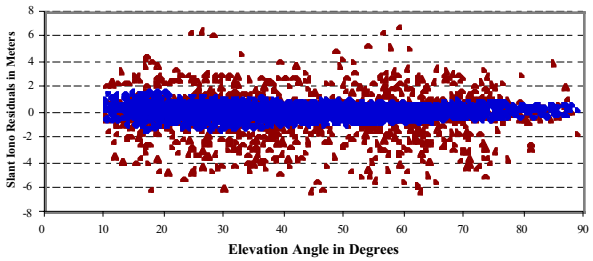

Figure 6. Elevation angle dependence of WAAS planar fit residuals for a typical CONUS (blue) and Brazilian (red) station for a quiet day, March 30, 2001.

Figures 5 and 6 show results from the quiet day of March 30. The subsequent day of March 31 turned out to be a day with a significantly disturbed ionosphere, corresponding to the largest geomagnetic storm of the year 2001. In the following sections we compare ionospheric model behavior between quiet and storm conditions.

Difference TEC map between quiet and storm days. To demonstrate the impact of storm activity, we have generated difference plots using all 230 stations processed for each day. The differences were formed on an individual slant TEC measurement basis, i.e., differencing the measurements between the quiet and storm days, using the same receiver observing the same satellite on the subsequent day minus 4 minutes to observe exactly the same geometry (correction for sidereal rotation). It is striking to see interday TEC differences as large as 60 TECU (9.6 meters on L1) in the middle of the CONUS sector, possibly indicating the presence of storm-enhanced densities (also known as SEDs) and depletions within CONUS [Foster et al., 2002].

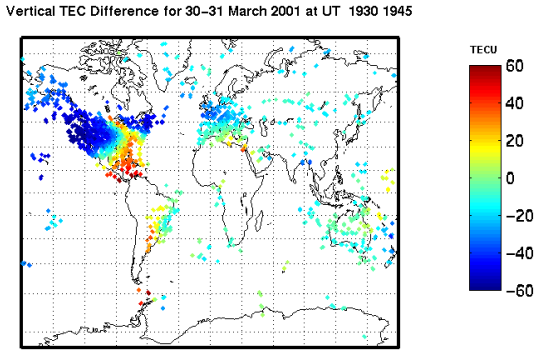

Figure 7. Difference map between two subsequent days (for UT interval 19:30 to 19:45) using unbiased slant measurements projected into the vertical.

In Figure 8, we have plotted the differences of slant ionospheric range delays between quiet and storm days for the CONUS station PRCO and Brazilian station UEPP. It is worth pointing out that for the CONUS region the differences turned out to be as high as they are for the

Brazilian sector. However, since CONUS delays are generally much lower than in Brazil, the relative impact of this storm in CONUS exceeded that in Brazil.

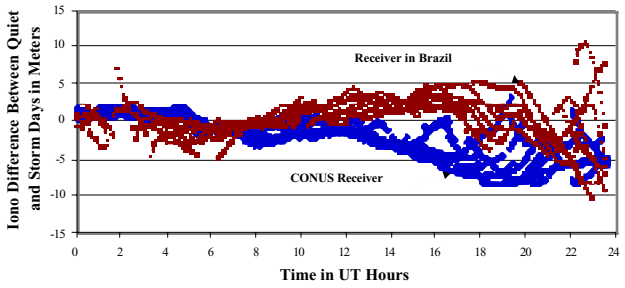

Figure 8. Differences between subsequent quiet (March 30) and storm day ionospheric slant delays (March 31) for typical CONUS and Brazilian stations.

Comparison of Brazilian residuals between quiet and storm days. In Figure 9, we display the Brazilian WAAS planar fit residuals for both quiet and storm days. Note that the behavior of the residuals is qualitatively similar. This suggests that the temporal and spatial variability of the equatorial anomaly may be masking the effects caused by the storm. This seems to be also supported by Figures 7 and 8 showing similar delay differences between quiet and storm in the CONUS and Brazil. Both for quiet and storm days, the magnitude of the Brazilian ionospheric residuals occasionally exceeded 18 meters.

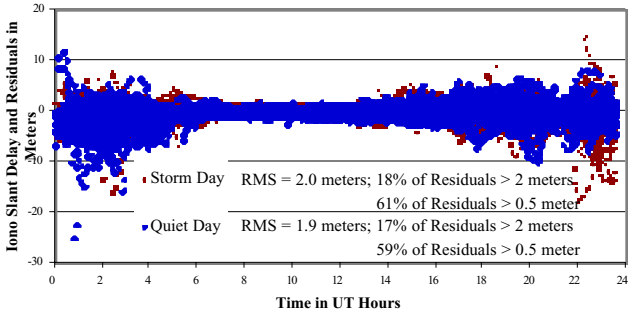

Figure 9. Brazilian planar fit slant-range residuals for quiet and storm days using 10 stations.

Comparison of CONUS residuals between quiet and storm days. The conclusion is slightly different when comparing the WAAS CONUS residuals between storm and quiet days. In Figure 10, it is evident that the storm contributed to higher residuals by more than a factor of three during UT hours 16 to 23 (Local Time (LT) corresponds to UT minus 3 hours). Slant residual magnitudes barely exceed 2 meters for the quiet day but reach nearly 8 meters for the storm day.

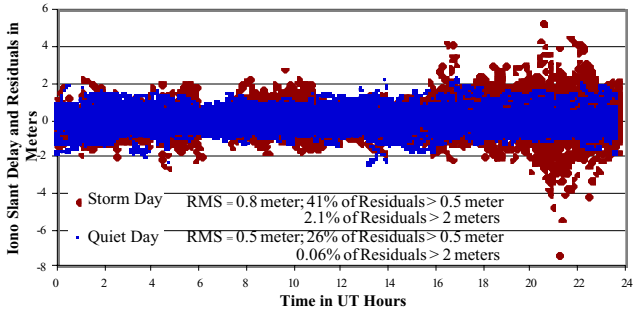

Figure 10. CONUS planar fit slant-range residuals for quiet and storm days using 10 CONUS stations.

Histogram of all planar fit residuals for storm day. We also computed histograms of all residuals for CONUS and Brazilian sectors. In Figure 11, note the difference in the shape of the distributions. The distribution of the Brazilian residuals is more similar to a double exponential and it is deviating from a typical Gaussian-shaped distribution. Similar conclusions were reached by Klobuchar et al., [2002] using simulated data points from the ionospheric models PIM and LowLat. We found the largest residual values of 18 and 7.5 meters for the Brazil and CONUS regions respectively. In the Figure 11, we used the same abscissa range (-10 to 10 meters) for CONUS and Brazil to reveal the different shape of the distributions. Neither distribution appears to be Gaussian probably due to highly varying ionospheric conditions that cannot be described by a simple Gaussian distribution. We note that careful interpretation is required when binning the residuals data for a single day while conditions are varying throughout the day, as occurs when the storm is present.

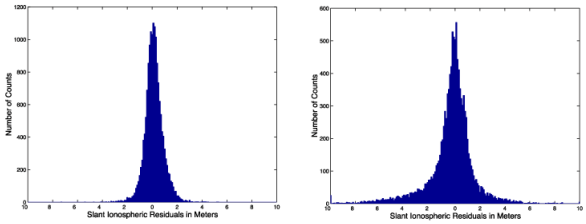

Figure 11. Histograms of storm-time slant delay residuals for the CONUS (left panel) and Brazilian (right panel) stations displayed.

Characterizing WAAS ionospheric delay differences. In Equation 2, it was shown that the WAAS algorithm estimates a constant term and slope terms in the East-West and North-South directions. To evaluate the WAAS planar fit performance further, we decided to take a closer look at the two gradient parameters estimated in the WAAS planar fit algorithm (Equation 2). We generated ground-truth by selecting pairs of stations observing the same satellites at nearly identical elevation and azimuth

angles. We computed vertical delay gradients by differencing the vertical TEC from these stations and tabulating the distance between them. The slant delays are converted to vertical using the WAAS obliquity scaling factor (thin shell at 350 km).

Delay difference between two receivers: time series at mid-latitude for quiet day. One such example is shown in Figure 12, displaying the difference between measured and estimated ionospheric delay for two receivers observing the same satellite at similar azimuth and elevation angle. After limiting the maximum separation between IPPs to 500 km, we found that the delay differences in CONUS can reach nearly 2.5 meters over 500 km for the quiet day. In Figure 12, we can clearly see the diurnal variation of the delay differences. The estimated delay differences usually overlap the measured values, indicating qualitatively that the actual delay differences are usually well-modeled by the fitted planar variation. However, we note larger discrepancies during the dawn and dusk hours where the temporal and spatial variability of the ionosphere is generally at its peak.

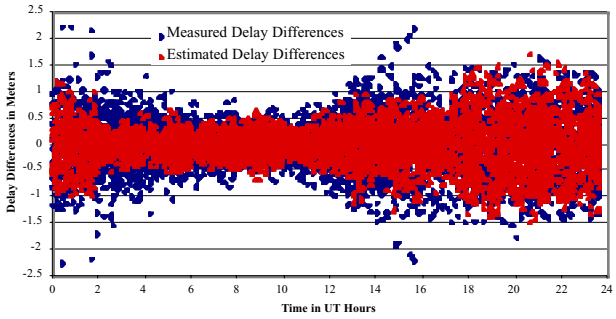

Figure 12. Measured (blue) and estimated (red) WAAS vertical delay differences for nearby receivers (spacing< 500km) for a CONUS quiet day.

Delay difference time series at mid-latitude for storm day. Figure 13 displays the measured and estimated delay differences for the storm day of March 31. The increased differences due to the storm is quite evident starting at about 16 hour UT (this corresponds to about 13 hour LT). Measured delay differences during the storm (over distances less than 500 km) reach as high as 6.5 meters. This is nearly a factor of 3 increase compared to the quiet conditions as depicted in Figure 12 (note the different vertical scales in the two figures). Not surprisingly, during the storm hours we also find larger discrepancies between the measured and estimated delay differences (shown in the figure as the vertical distance between the blue dots and corresponding red dots). The largest difference between measured and estimated gradient was 5 meters at 21 hours UT over a distance of 480 km.

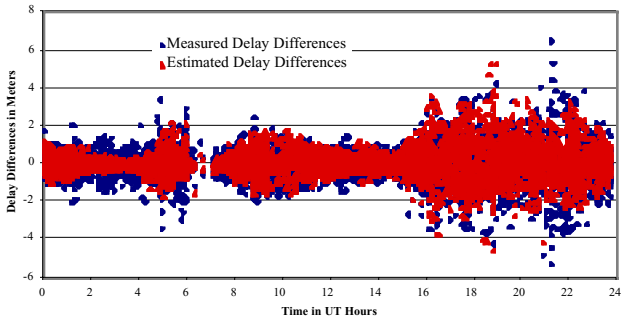

Figure 13. Measured and estimated vertical delay differences for a CONUS storm day.

Delay difference distance dependence at mid-latitude for quiet day. In Figure 14, we display measured and estimated delay differences as a function of distance between two observations at nearly identical elevation and azimuth angles. In this figure we have separately plotted the delay differences in terms of longitudinal ($a_1 d_E$) and latitudinal ($a_2 d_N$) components as estimated by the planar fit algorithm in Equation 2. As expected the latitudinal (North-South) components dominate the delay differences. For the quiet day we found that ionospheric gradients along the North-South direction did not exceed 0.5 meters over 100 km (2.5 meters over 500 km as shown in the figure). Some of the larger differences between the measured and estimated delay differences correspond to dawn and dusk periods as was shown in Figure 12.

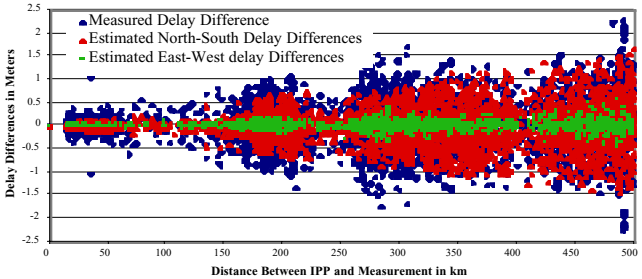

Figure 14. Vertical delay differences as a function of distance for a CONUS quiet day.

Delay difference distance dependence at mid-latitude for storm day. For the storm day in Figure 15, we found that the North-South gradients were bounded by 1.2 meters over 100 km (or 6 meters over 500 km), which represents more than a factor of 2 increase compared to the quiet day conditions. Note also the increased contribution of the longitudinal gradient, suggesting more complex structures in the mid-latitude ionosphere as we already noticed a significant increase in the RMS of residuals compared to the quiet day conditions.

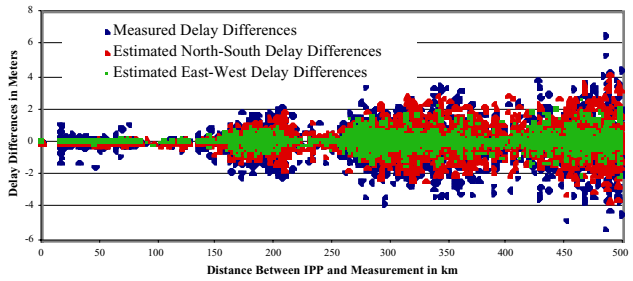

Figure 15. Vertical delay differences as a function of distance for a CONUS storm day.

Elevation angle times series. In Figure 16, we have plotted the delay differences as a function of elevation angle. It appears to indicate no elevation angle dependence which is what we expected, providing evidence that the selection of pairs of stations with nearly identical elevation and azimuth angles are performed with sufficiently tight tolerances (elevation angle tolerance less than 2 degrees, azimuth angle tolerance less than 30 degrees). To obtain sufficient numbers of observation pairs, the elevation and azimuth tolerances should not be overly restrictive. Stringent elevation and azimuth angle tolerance results in small number of observation pairs while observations with loose tolerances would no longer represent the same geometry that we wish to take advantage of.

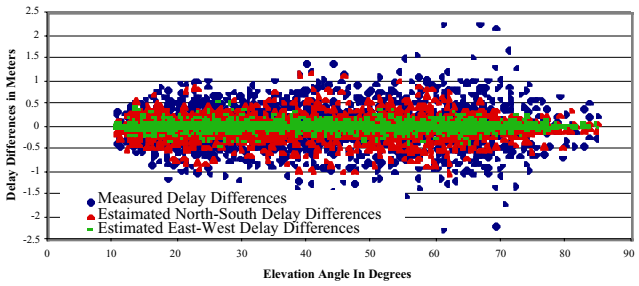

Figure 16. Elevation angle dependence of the delay differences for the quiet day of March 30, 2001. Weak dependence suggests that the azimuth/elevation tolerances are not too loose.

Delay difference time series at low-latitude for quiet day. Figure 17 shows the measured and estimated vertical delay differences for the Brazilian sector during a quiet day. The discrepancy between the measured and estimated delay differences are more evident than they are for the CONUS sector. Even for the quiet day (see Figure 17), we detect large discrepancies in the measured and estimated delay differences during 20 to 06 hours UT. The overall RMS of measured and estimated range delay differences turned out to be 1.9 meters. Note that the current distribution of GPS sites in Brazil results in a smaller number of observations meeting the criteria of two observations being at nearly the same elevation and azimuth angles, compared to the better spatial distribution of CONUS receivers.

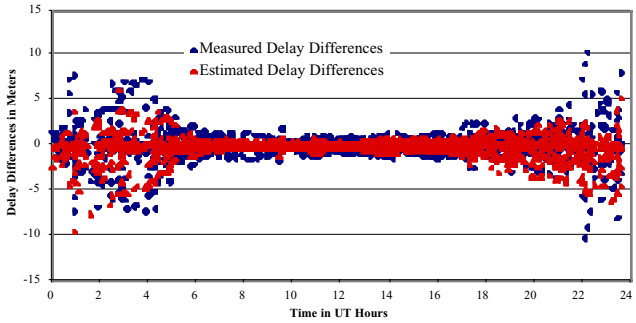

Figure 17. Measured and estimated vertical delay differences for Brazil during a quiet day.

Delay difference times series at low-latitude for storm day. After performing the same comparison for a storm day, Figure 18 shows interesting results i.e, we do not see a major impact of the storm. The overall structure of the delay differences is very similar to that for the quiet day; the RMS of slant residual differences between measured and estimated values is 2.0 meters.

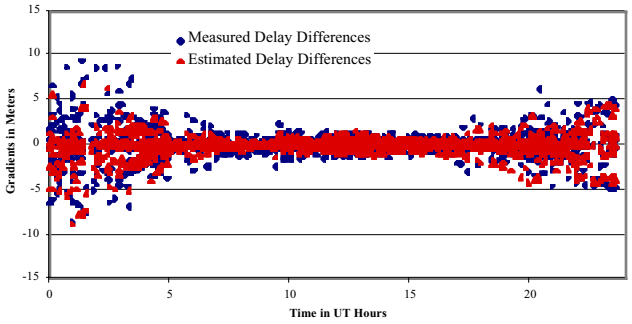

Figure 18. Measured and estimated delay differences for Brazil during a storm day.

Delay difference distance dependence at low-latitude for quiet and storm days. To see a complete picture, in Figures 19 and 20, we have plotted the delay differences as a function of distance between the two points used in the gradient calculation. For the quiet and storm days, we observe similar delay differences that are as high as 10 meters over 500 km (2 meters over 100 km). In the figures we see three groups of data points. This discontinuity is related to the uneven geographical distribution of the GPS sites in Brazil.

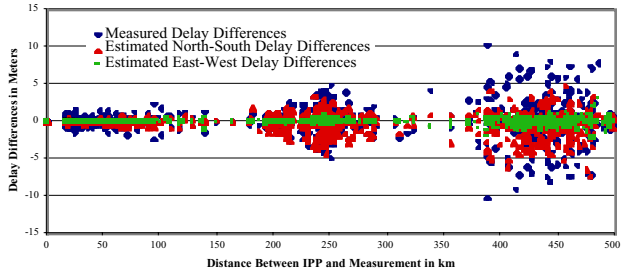

Figure 19. Vertical delay differences as a function of distance for Brazil during a quiet day.

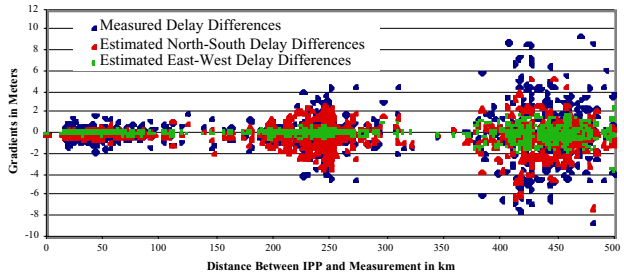

Figure 20. Vertical delay differences as a function of distance for Brazil during a storm day.

Mapping function error. As another potential error source, we explored the errors introduced by the thin-shell ionospheric mapping function. The idea is to find pairs of observations from different receivers with nearly co-located IPPs. If the elevation mapping function contains no errors, the two slant observations should provide us with identical vertical range delays. In fact, mapping function errors are present and assessed by projecting the two slant observations into the vertical using the respective elevation angles and subsequently taking the difference between the two nearly collocated vertical estimates. In Figure 21, we show the elevation angle dependence of the mapping function errors for CONUS and Brazil (elevation angle of the pseudo-IGP used for plotting). For CONUS, the errors never exceed 2 meters. For the Brazil sector, the error can exceed 8 meters.

The highest value for mapping function error (as high as 8 meters) is consistent with the maximum error of -13.4 meters obtained by Klobuchar et al., [2002] using simulated data down to 5 degree elevation cutoff angle. In our study, we used 10 degree elevation cutoff angle. The statistics we computed refer to mapping function errors in vertical delay. One would need to multiply the errors by an average factor of about 2 (a factor of 3 at 10 degree elevation angle) to compute slant delay errors due to the mapping function.

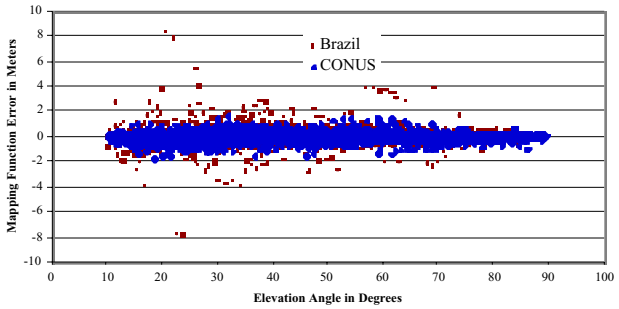

Figure 21. Mapping function errors for CONUS and Brazil as a function of elevation angles.

Implications for LNAV/VNAV availability. We have investigated ionospheric range errors in the mid-latitude CONUS and low-latitude Brazilian sectors for quiet and storm days. Based on this limited data set, we found that using a tuned variant of the WAAS planar fit algorithm, we were able to achieve better than 0.5 meter RMS ionospheric slant delay residuals for the quiet day and 0.8 meter for the storm day in the CONUS. For the Brazilian sector, the quiet day produced RMS residuals of 1.9 meter in slant delay and 2.0 meters for the storm day.

The quiet-time CONUS results are reasonably consistent with what has been observed in previous analyses of ionospheric residuals to the planar fit for quiet conditions [Walter et al., 2000]. Residuals in Brazil are approximately a factor of four larger on average. This has major implications for availability of the initial WAAS Lateral Navigation/Vertical Navigation service (LNAV/VNAV). The user determines, in real-time, the level of navigation service available based on the broadcast grid ionosphere vertical errors (GIVEs) and other information. GIVE values represent 3.29-sigma bounds on vertical ionosphere range error at each ionospheric grid point. Service volume model studies for WAAS have shown that high availability of LNAV/VNAV service is possible when a significant majority of the broadcast GIVEs are in the range 3-6 meters. This performance is expected for WAAS.

At low latitudes, the GIVEs must be increased to cover the larger ionospheric range errors expected. Increased planar fit residuals by a factor of four are likely to result in a substantial number of GIVEs above 6 meters. Due to GIVE quantization in the broadcast message, computed GIVEs above 6 meters are transmitted as 15-meter bounds to the user. It is clear that LNAV/VNAV service will be unavailable if several of the user s satellite links are associated with GIVEs of 15 meters or more.

We expect that the WAAS planar fit algorithm applied to Brazil will result in significantly reduced availability of LNAV/VNAV service, particularly near solar maximum

during daytime and evenings. Additional factors, such as the possible presence of plasma bubbles observed in the equatorial region [Dehel and Corbelli, 2002] will further contribute to much larger GIVE values in Brazil compared to CONUS.

CONCLUSIONS AND FUTURE RESEARCH

In this paper, we have compared the performance of the WAAS ionospheric planar-fit correction algorithm in the CONUS and Brazilian sectors for both quiet and storm days from recent high solar activity periods. We used data from a network of dual-frequency GPS receivers in the mid-latitude CONUS and Brazilian sectors. Unbiased line-of-site TEC ground-truth data were generated using JPL s Global Ionospheric Mapping (GIM) software. Using the truth data, the WAAS planar fit algorithm was evaluated by treating each observation as representing a WAAS ionospheric grid point (IGP) and computing the planar fit estimate for that IGP after excluding it from the fit.

We found slant ionospheric range delays up to 30 meters for day-time CONUS and as high as 60 meters for Brazil. For the quiet day, we obtained WAAS planar fit residuals less than 2 meters (0.5 meter RMS) for CONUS and usually less than 15 meters (1.9 meter RMS) for Brazil. For the storm day, the WAAS planar fits resulted in less than 8 meters (0.8 meter RMS) residuals, compared to the Brazilian residuals which are up to 18 meters (2.0 meters RMS). It is interesting to see that the storm had a small impact on the planar fit residuals in the Brazilian sector compared to quiet conditions. However, the storm effect was more pronounced in the CONUS region.

For CONUS, we found ionospheric gradients, averaged over distances of a few hundred km, were no larger than 0.5 meter per 100 km for quiet conditions, and no larger than 1.2 meters over 100 km for storm day. For Brazil, we observed gradients as large as 2 meters over 100 km both for quiet and storm days. Studies by Dehel and Corbelli [2002] found gradients in Brazil similar or even larger in size associated with plasma bubbles typically appearing after sunset during solar maximum.

Errors associated with mapping slant observations to vertical occasionally resulted in errors of about 8 meters (vertical) in Brazil. In CONUS, these errors never exceeded 2 meters on the processed day.

This investigation has addressed only some of the difficulties the user will face in the Brazilian sector using the current WAAS algorithm. It appears that the inherent spatial variability of the ionosphere is driving the residual errors seen at low-latitude. Other influencing factors such as bubbles and plumes have not been addressed in this paper. Since the data sets we analyzed represented high solar activity quiet and storm time conditions, the results may also be considered to be upper bounds for medium and low solar activity conditions.

We are currently looking at other alternative algorithms to augment or replace the WAAS algorithm in Brazil. This will include fitting higher order surfaces to the data. Initial assessment of fitting a quadratic surface to the data provides us with only marginal improvement in accuracy. In addition to large ionospheric delays and gradients in the equatorial region, users will also be exposed to 15-20 meter level large depletions or bite-outs due to plasma bubbles [Dehel and Corbelli, 2002]. We are planning on evaluating these effects and determining the density of ground stations necessary to detect these structures so that full integrity of the corrections is maintained.

Previous studies of ionospheric decorrelation have relied on so-called WAAS supertruth data derived from collocated GPS receivers to robustly detect anomalies in the data. In the absence of Brazilian supertruth data, this research was conducted using dual-frequency GPS data from CORS, IGS and Brazilian sites with no redundant observations available.

With no redundancy, robust data editing algorithms were applied to remove outliers, but it is possible that some valid data was rejected, or marginally poor data was accepted. Preprocessing of the raw data was conducted with scrutiny making sure that the data editing algorithm did not eliminate large numbers of observations. Consideration of the number of accepted points between the two days suggests that data editing has not played a significant role in this study. Based on our analyses, we expect that data editing played at most a minor role in the conclusions drawn so far. This question will be further confirmed in the future.

ACKNOWLEDGMENTS

This research was performed at the Jet Propulsion Laboratory/California Institute of Technology under contract to the National Aeronautics and Space Administration and the Federal Aviation Administration. We greatly appreciate the help from Dr. Eurico de Paula and Mariangel Fedrizzi (both at the Instituto Nacional de Pesquisas Espaciais, INPE) for providing us with the GPS data from Brazil.

REFERENCES

Blanch, J., T. Walter and P. Enge. (2002). Application of Spatial Statistics to Ionosphere Estimation for

WAAS. *On the CD-ROM of the Proceedings of the National Technical Meeting of the Institute of Navigation*, San Diego, CA, January 28-30.

CORS (2002). Continuously Operating Reference Stations, http://www.ngs.noaa.gov/CORS/, Accessed 10 August.

Dehel T. and M. Corbelli (2002). Brazilian Test Bed: Ionospheric Analysis. Presented at the ATN/GNSS CAR/SEM Seminar, Varadero, Cuba, 6-9 May, http://www.icao.int/nacc/meetings/atngnss2002/gnss_71b2_brazil.pdf.

Enge, P., T. Walter, S. Pullen, C. Kee, Y.C. Chao and Y.-J. Tsai (1996). Wide Area Augmentation of the Global Positioning System. *Proceedings of the IEEE*, Vol. 84, pp. 1063-1088.

Fedrizzi, M., R.B. Langley, A Komjathy, M.C. Santos, E.R. de Paula, I.J. Kantor (2001). The Low-Latitude Ionosphere: Monitoring Its Behavior with GPS. *On the CD-ROM of the Proceedings of ION GPS 2001, 14th International Technical Meeting of the Satellite Division of The Institute of Navigation*, Salt Lake City, UT, 11-14 September.

Foster, J. C., P.J. Erickson, A.J. Coster, J. Goldstein and F.J. Rich (2002). Ionospheric signatures of plasmaspheric tails. *Geophysical Research Letters*, Vol. 29, No. 15.

Hansen, A.J., T. Walter and P. Enge (1997). Ionospheric Correction Using Tomography. *Proceedings of ION GPS-97, the 10th International Technical Meeting of the Satellite Division of The Institute of Navigation*, Kansas City, MO, U.S.A., 16-19 September, pp. 249-257.

IGS (2002). International GPS Service, http://igscb.jpl.nasa.gov/, Accessed 5 September.

Iijima, B.A., I.L. Harris, C.M. Ho, U.J. Lindqwister, A.J. Mannucci, X. Pi, M.J. Reyes, L.C. Sparks, B.D. Wilson (1999). Automated Daily Process for Global Ionospheric Total Electron Content Maps and Satellite Ocean Altimeter Ionospheric Calibration Based on Global Positioning System. *Journal of Atmospheric and Solar-Terrestrial Physics*, Vol. 61, pp. 1205-1218.

Klobuchar, J.A., P.H. Doherty, M. Bakry El-Arinim R. Lejeune, T. Dehel, E.R. de Paula and F.S. Rodriges (2002). Ionospheric Issues for a SBAS in the Equatorial Region. *Proceedings of the 10th International Ionospheric Effects Symposium*, 7-9 May.

Komjathy, A. (1997). *Global Ionospheric Total Electron Content Mapping Using the Global Positioning System*. Ph.D. dissertation, Department of Geodesy and Geomatics Engineering Technical Report No. 188, University of New Brunswick, Fredericton, New Brunswick, Canada, 248 pp.

Komjathy, A., B.D. Wilson, T.F. Runge, B.M. Boulat, A.J. Mannucci, L. Sparks and M.J. Reyes (2002). A New Ionospheric Model for Wide Area Differential GPS: The Multiple Shell Approach. *On the CD-ROM of the Proceedings of the National Technical Meeting of the Institute of Navigation*, San Diego, CA, January 28-30.

Lawson, C. (1984). A Piecewise C2 Basis for Function Representation over a Surface of a Sphere. JPL internal document.

Mannucci, A.J., B.D. Wilson, D.N. Yuan, C.H. Ho, U.J. Lindqwister and T.F. Runge (1998). A Global Mapping Technique for GPS-derived Ionospheric Total Electron Content Measurements. *Radio Science*, Vol.33, pp.565-582.

Mannucci A.J., B.A. Iijima, L. Sparks, X. Pi, B.D. Wilson and U.J. Lindqwister (1999). Assessment of Global TEC Mapping Using a Three-Dimensional Electron Density Model. *Journal of Atmospheric and Solar Terrestrial Physics*, Vol. 61, pp. 1227-1236.

Sparks, L., B.A. Iijima, A.J. Mannucci, X. Pi, B.D. Wilson (2000). A New Model for Retrieving Slant TEC Corrections for Wide Area Differential GPS. *Proceedings of the ION National Technical Meeting 2000 of the Institute of Navigation*, Anaheim, CA, 26-28 January, pp. 464-474.

Sparks, L, A. Komjathy and A.J. Mannucci (2002). Sudden Ionospheric Delay Decorrelation and Its Impact on WAAS. *Proceedings of the 10th International Ionospheric Effects Symposium*, 7-9 May.

WAAS MOPS (1999). Minimum Operational Performance Standards for Global Positioning System/Wide Area Augmentation System Airborne Equipment. RTCA Inc. Document No. RTCA/DO-229B October 6. pp 225.

Walter, T., A. Hansen, J. Blanch, P. Enge, T.J. Mannucci, X. Pi, L. Sparks, B. Iijima, B. El-Arini, R. Lejeune, M. Hagen, E. Altschuler, R. Fries, A. Chu (2000). Robust Detection of Ionospheric Irregularities. *On the CD-ROM of the Proceedings of ION GPS 2000, 13th International Technical Meeting of the Institute of Navigation*, Salt Lake City, UT, 11-14 September.